Available online at www.sciencedirect.com

ScienceDirect

Procedia Structural Integrity 12 (2018) 429–437

Structural Integrity Procedia

www.elsevier.com/locate/procedia

AIAS 2018 International Conference on Stress Analysis

Analysis of bistable composite laminate with embedded SMA actuators

Yogesh Gandhi[a,*], A. Pirondi[a], L. Collini[a]

[a]*Dipartimento di Ingegneria e Architettura, Università di Parma, Parco Area delle Scienze, 181/A, Parma 43124, Italy*

Abstract

The present work is aimed at the development of a finite element model of a composite laminate, to evaluate the possibility to snap between equilibrium configurations by means of shape memory alloy (SMA) wires. The underlying idea is to potentially take advantage of structures which possess multiple equilibrium configurations that can be achieved with a small energy input. Therefore, unsymmetric composite laminates that exhibit bistable response to actuation force are considered. Embedded SMA wires will provide the actuation force by virtue of Shape-Memory Effect i.e. restoring the original shape of a plastically deformed SMA wire by heating it. The Shape-Memory Effect is modelled in a simplified way using the Effective Coefficient of Thermal Expansion concept.

Keywords: shape memory alloy cross-ply laminate; snap-through; shape memory effect; bistable structure.

1. Introduction

The demanding need for better performance of fixed-wing aircraft, rotorcraft and spacecraft has obviously appeal an interest in adaptive or morphing structural systems which are capable of significant shape change. The bistability behaviour of unsymmetric laminate motivated researchers to exploit this characteristic in numerous aerospace applications. Examples are: i) the use of Morphing Wingtip device whose benefit (in term of induced drag

* Corresponding author. Tel.: +39-320 235 3270.
E-mail address: yogesh.gandhi@unipr.it

10.1016/j.prostr.2018.11.075

reduction) offset the penalties (extra cost and weight) as shown by Büscher et al. (2006); ii) the development of a variable geometry airfoil which effectively changed its configuration from symmetric to cambered by J. K. Strelec et al. (2003); iii) the use of SMA torque tubes to vary the twist of rotor blades proposed by A. Jacot et al. (2006).

Unsymmetric composite laminates can develop a residual stress field when subjected to a thermal field due to mismatch in coefficient of thermal expansion in an unsymmetric stacking sequence. Such a laminate configuration is of interest since out-of-plane displacement can be achieved through generation of bending and twisting moments with respect to mid-plane, resulting in internal stress equilibrium at a new stable configuration. This behaviour of unsymmetric laminates to exhibit two stable equilibriums and to settle at either of them by overcoming the 'energy barrier' between two states is a common example of bistability of structure. The intrinsic anisotropy of composite structures was first exploited by Hyer (1981) using unsymmetric layups to produce bi-stable morphing structure at room temperature. Jun and Hong (1990) modified Hyer's theory by taking in account in-plane shear strain whereas, Dang and Tang (1986) included higher order polynomial to calculate displacement field respectively. Despite these complex modifications, there were no significant improvements to the results.

Schlecht and Schulte (1999) firstly provided the bi-stable behaviour of asymmetric laminates using MARC Finite Element Analysis (FEA) software. Tawfik et al. (2005) presented a finite element approach using ABAQUS™ to predict the unsymmetric laminate shapes under thermal curing stresses. In the finite element software ABAQUS, two ways are available to follow unstable, therefore non-converging analyses, namely the "RIKS" algorithm and the "Stabilize" option. The "RIKS" algorithm, considers the load magnitude as an additional unknown; it solves simultaneously for loads and displacements and predict the entire nonlinear behaviour in the case of load reversal. On the other hand, the Stabilize option stabilizes quasi-static problems through the automatic addition of volume-proportional damping to the model. In general, if the stabilize option is very effective in solving localized instabilities rather than global, although Mattioni et al. (2008) pointed out that it is suitable also for snap-through problems such unstable-stable configuration change in $[0_n/90_n]$ laminates.

Shape memory alloys (SMA) have good characteristics as actuators by exhibiting the *shape memory effect* (SME), which can generate a significant actuation force due to phase transformation during strain recovery from the martensitic phase at a low temperature to the austenitic phase at a high temperature. The concept of embedding SMA actuation in a composite structure was introduced by Rogers and Robertshaw (1988). Ryu et al. (2011) verified actuation of asymmetric laminate using SMA spring actuator through the comparison between experiment and numerical simulation. Dano and Hyer (2003) used a mechanism wherein, after SMA wires were stretched between a system of support above the laminate and upon electrical heating of the SMA wires, it could generate enough force to pull the tips of the supports toward each other, thereby cause the laminate to snap. The major underside was the arrangement looks like cumbersome and impractical.

The objective here is to evaluate the possibility to trigger the snap-through from one stable configuration to another by means of shape memory alloy (SMA) wires embedded into the laminate. The underlying idea is to potentially take advantage of structures which possess multiple equilibrium configuration and stable configurations can be achieved with small and removable energy input. The actuation mechanism employed by the laminate in this study increase the potential energy of the bi-stable laminate, by elevating the temperature of Embedded SMA wires which will exhibit Shape-Memory Effect i.e. restoring the original shape of a plastically deformed SMA wire by heating it.

2. Bistable laminates

If a negative temperature difference is imposed on a $0_n/90_n$ laminate, as, the 90° plies tend to "shrink" more than the 0° plies. To satisfy compatibility of displacements, for a perfect interface the laminate will develop a curvature to counter effect the residual stresses associated with the inability of each layer to freely stretch by the given amount. According to the classical lamination theory, this out-of-plane deflections results in a saddle configuration. However, this is true only with thick laminates but for thin laminates two statically stable cylindrical equilibrium configurations exist, and the laminate is thus often termed as being bistable as depicted in Fig. 1. The existence of bistable configuration depends on the overall dimension of the laminate, layer stacking sequence and material properties, including the thermal expansion characteristics.

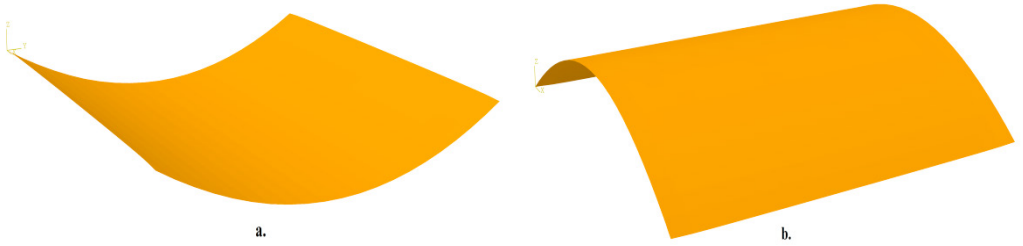

Fig. 1. Bistable Laminate: a) 1st Cylindrical Shape with curvature in y-direction; b) 2nd Cylindrical Shape with curvature in x-direction.

As the laminate cools down from the curing temperature, it acquires a curvature dominated by the thermal strain of one of the layers. However, significant residual stress will be present associated with the thermal strains of other layers and if an appropriate load is applied to the laminate, this latter will acquire a curvature dominated by the thermal strains of those other layers (Luìs Falcã et al. (2007)). Due to this behaviour, the unsymmetric laminate can be changed from the one stable configuration (curvature) to the other with small and removable actuation force.

In this work, the laminate is modelled in ABAQUS with the composite option to create 4-ply within the thickness of the shell element. Each ply is of equal thickness and the stacking sequence of laminate is $[0_2/90_2]$. The material taken for modelling is a carbon-epoxy composite manufactured by NorthTPT, Renens. It is made of high modulus Toray M40JB carbon fibres and an 80°C curing temperature epoxy resin called TP80EP. The tabulated coefficient of thermal expansions in table 1 are assumed value for carbon/epoxy composite.

Table 1. Orthotropic material properties for M40JB fibres and ThinPreg™ 80EP/CF epoxy resin.

E_{11} (GPa)	E_{22} (GPa)	G_{12} (GPa)	ν_{12}	α_{11}/°C	α_{22}/°C	t_{ply} (mm)
222	7.01	4.661	0.314	0.21E-06	29.8E-06	0.075

3. Shape Memory Alloy

Shape Memory Alloy can exist in two distinct phases, each with different crystal structures and therefore different mechanical properties. The two different temperature-dependent phases are austenite at high temperatures and martensite at low temperatures. The reversible phase transformation between these two phases forms the basis for the unique behavior of SMAs. If temperature is decreased, under zero load, austenite completes *forward transformation* to twinned martensite at the martensite final temperature (M_f), Similarly, during heating, *reverse transformation* reverts to the parent phase (austenite) at the austenite final temperature (A_f). When the twinned martensite is subjected to mechanical load, it possible to reorient martensite variants such that it results in macroscopic shape change, where the deformed configuration is retained when the load is released. This process to detwin martensite variant results in detwinned martensite.

3.1 Shape Memory Effect

The unique behaviour of SMAs exhibits the Shape Memory Effect when twinned martensite phase is deformed below M_f or at a temperature between M_f and A_s (austenite starting temperature), above which the martensite becomes unstable. Thus, if the external load is released, while at a temperature below A_s and when SMA is heated to a temperature above A_f, reverse transformation occurs i.e. SMA returns to its original shape of the austenite phase. The described phenomenon, where the shape of austenite phase is remembered called as *one-way shape memory effect* (OWSME). However, a trained SMA can remember the shape of the martensite phase and exhibit reversible shape changes between two different phases under no mechanical load when subjected to a thermal load. This effect is termed as *two-way shape memory effect* (TWSME). For further reading referred to the book by Lagoudas et al. (2008).

3.2. ECTE model for SMA

A model is needed to describe the SME behaviour of SMA wires that is accomplished here by a constitutive model based upon nonlinear thermo-elasticity and the definition of an effective coefficient of thermal expansion (ECTE) as proposed by Turner et al. (2007). The fundamental feature of the ECTE model is the axial constitutive relation for a SMA actuator, in which the non-mechanical (i.e., thermal and transformation) strains below the austenite start temperature ($T<A_s$) is represented by effective thermal strain:

$$\sigma_{1a}(T) = E_a(T)[\varepsilon_1 - \int_{T_0}^{T} \alpha_{1a}(\tau)d\tau] \tag{1}$$

where E_a is the Young's modulus of the SMA material, ε_1 is the total axial strain of SMA-Composite Structure, α_{1a} is the effective coefficient of thermal expansion, and the subscript a indicates that the quantity is specific to the actuator material. It can be seen in Equation 1 that the ECTE model is intended to model thermally induced transformation phenomena, as opposed to stress induced (pseudo-elasticity), which is the restriction on ECTE model. It can be shown that the thermal strain in Equation 1 is governed by the usual thermoelastic effects at temperatures below the austenite start temperature and is related to the recovery stress at higher temperatures:

$$\sigma_{1a}(T) = -E_a(T)\int_{T_0}^{T} \alpha_{1a}(\tau)d\tau \quad or \quad \int_{T_0}^{T} \alpha_{1a}(\tau)d\tau = -\sigma_r(T)/E_a(T) \tag{2}$$

The ECTE model was developed by Turner et al. to simulate a SMA Hybrid Composite (SMAHC) laminate where equations 1 or 2 where used, along with the corresponding ones for the transverse strains to build up the reduced stiffness matrix terms of the SMAHC ply, Q_{ij}, and the thermoelastic effective strains (more details about the model can be found in the study by Turner et al. (2007)). In this work, the use of the ECTE model has been restricted to the axial direction to provide the stress-strain behaviour of SMA wires in a simplified manner that can be dealt with using the Abaqus™ software without any user-defined routine. Temperature-dependent orthotropic material properties for Nitinol are provided in table 2.

Table 2. Temperature-dependent material properties for Nitinol (Turner et al. (2007)).

Temperature, °C	α_{11}/°C	E_{11}, Pa	ν_{12}
16	6.61E-06	27170	0.3
21	6.61E-06	27170	0.3
27	-3.09E-05	24800	0.3
32	-3.87E-05	22430	0.3
38	-5.04E-05	20060	0.3
43	-5.57E-05	25700	0.3
49	-1.01E-04	31340	0.3
54	-1.35E-04	36890	0.3
60	-1.42E-04	42620	0.3
66	-1.34E-04	48270	0.3
71	-1.20E-04	54860	0.3
77	-1.05E-04	61450	0.3
82	-9.93E-05	64210	0.3
88	-9.90E-05	63130	0.3
93	-9.72E-05	62060	0.3
99	-9.13E-05	63920	0.3

3.3. Nitinol wire as an actuator

The shape memory effect of SMAs to remember a predetermined shape even after large inelastic deformation nominated SMAs as a suitable candidate for actuation application. For one-time actuation application, one can utilize maximum attainable actuation strain for a given alloy, i.e., up to 8% for Nitinol (NiTi). However, for repetitive actuation, lower transformation strains are preferred as to increase fatigue life and decrease plastic strain development. Based on that, a notion can be developed to snap unsymmetric laminate to either of its stable configuration as desired, by embedding SMA wires inside the laminate. The aim of this work is to take benefit from SME behaviour of NiTi wires in pursuance to harvest enough actuation force such that the laminate can snapped from its 1st statically stable configuration (cured shape) to 2nd statically stable configuration. This work considers NiTi wires that can exhibit TWSME, thus eliminating the need to pre-stretch them -contrary to OWSME. Moreover, consideration should be taken on the austenite final temperature of actuators such as to keep it well above the curing temperature to avoid coupling of two processes, namely cool-down stage and actuation stage (TWSME). During cool-down stage, actuators initially undergoes thermal contraction and in addition to that axial compressive stress also arises in wires to accommodate the laminate's curvature (1st Cylindrical State) as temperature is brought down to the ambient temperature. This step facilitates elastic deformation in NiTi wires, which will depend on the curvature acquired by the laminate. In actuation stage, NiTi wires subsequently heated above A_s and wires will start regaining their original shape by transforming back into the parent austenite phase. This result in actuation (contraction) of NiTi wires and above A_f, the actuation is complete, and the wires return to their parent phase. The process of phase transformation or TWSME is based on the ECTE model (section 3.2) and forms the basis to attain the 2nd statically stable state through snap-through event.

4. FEA of snap-through behavior of an unsymmetric composite laminate

4.1. Finite Element Model and setup

In this section, the commercial finite element code ABAQUS was employed to simulate the snap-through of the bi-stable laminate using actuation force generated by SMA wires embedded in the laminate. A 75 x 75 mm^2 laminate was modelled in ABAQUS using 4-node, reduced integration shell elements S4R with 4-plies and a $[0_2/90_2]$ stacking sequence. General-purpose shell elements, such as S4R, have more robust convergence properties in heavily non-linear simulations. The embedded SMA wires is modelled using T3D2 truss elements such that the nodes of SMA wires coincide with the nodes of the laminate and a tie constraint is established between the node region of SMA wires and laminate as depicted in Fig. 2b. As a truss element has only axial degrees of freedom they can carry only axial loads alike thin, flexible NiTi wires. The Finite Element mesh consists of 400 linear quadrilateral elements of type S4R and 200 linear line elements of type T3D2 (Fig. 2c).

To set the initial stage, the shape of laminate is obtained by cooling down from curing temperature of 80°C to room temperature of 21°C. However, based on the work of Koiter (1967), large discrepancies between theoretical and experimental results may occur due to imperfections always present in actual structures. Therefore, the saddle shape retrieved numerically after cooling may not be found in practice but one of the other two stable cylindrical shapes manifests instead. To manage this point, an initial imperfection is introduced on the 'perfect' laminate structure as a scale factor equal to one tenth of the laminate thickness of the first three eigenmodes obtained by a preliminary eigenvalue buckling analysis performed under a thermal load that correspond to the curing cycle and in this way, the 1st *Cylindrical State* is retrieved. During the cool-down stage, the laminate embedded with SMA wires is "ENCASTRE" at the centre node of laminate and the temperature is uniformly brought down to room temperature. The dissipated energy fraction of 0.0002 for stabilization is set to reduce the local instability in the snap simulation. Note that table 2 represent the model for SME behaviour, where α_{1a} based on the recovery stress and not an actual coefficient of thermal expansion for NiTi wires. For this reason, approximate material properties for NiTi wires used during cool-down stage are shown in table 3.

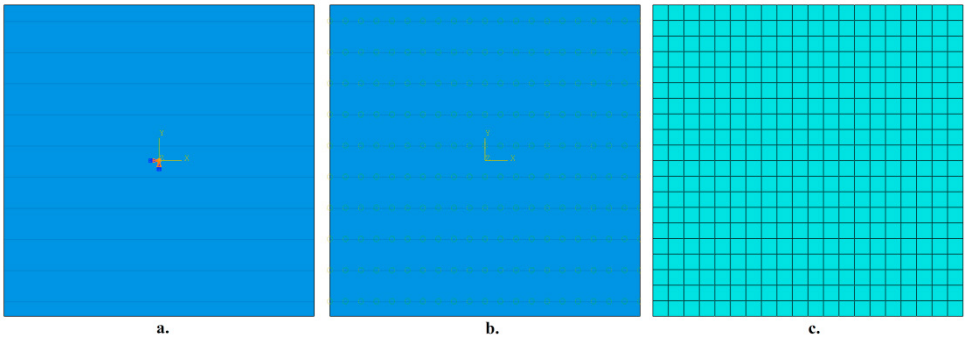

Fig. 2. a) Boundary Conditions; b) Tie constraint between trusses (SMA wires) and shell (composite); c) Finite Element Mesh.

After the cool-down stage simulation, the snap-through event of the laminate is modelled by heating NiTi wires to generate the actuation force. After several trial-and-error analyses, ten Nitinol wires (Ni: 50.4 wt%, Ti: 49.6 wt%) with a diameter of 200μm diameter arranged on the laminate as shown in Figure 2a and the transformation temperatures (TTRs) A_s = 70.5°C, A_f = 96.9°C, M_s = 62.7°C, and M_f = 17.4°C are considered due to compatibility with a cure temperature of the present laminate. In this work, it is assumed that the TTRs of NiTi wires independent of wire diameter since these determined TTRs were measured by Jung et al. (2010) with a diameter of 400μm. The setup for the snap-through event to attain 2nd *Cylindrical State*, the boundary conditions is modified such that "ZAYSMM" is assigned to centre node instead of the "ENCASTRE" restraint. The wires are actuated by elevating their temperature to 96.7°C, this result in the load transfer from the longitudinal contraction of embedded nitinol wires to the laminate via interfacial shear. This provides a means to generate actuation force to overcome the "energy barrier" between two stable configurations of unsymmetric laminate. To evaluate if laminate will retain a stable configuration, the NiTi wires finally cool down to the ambient temperature.

Table 3. Material Properties for Nitinol during the cool down stage from cure temperature (Lagoudas et al. (2008)).

α_M/°C	E_M (GPa)	ν_M
10.0E-06	30	10.0E-06

4.2. Results

The obtained stable configuration of the laminate embedded with NiTi wires after the curing and actuation stage is shown in Fig. 3. The 2nd cylindrical stable shape, is obtained by the suitable placement of actuators on the laminate and the minimum number of wires required for a given wire size, yielded the snap from the 1st to the 2nd cylindrical state of the laminate as depicted in Fig. 3b.

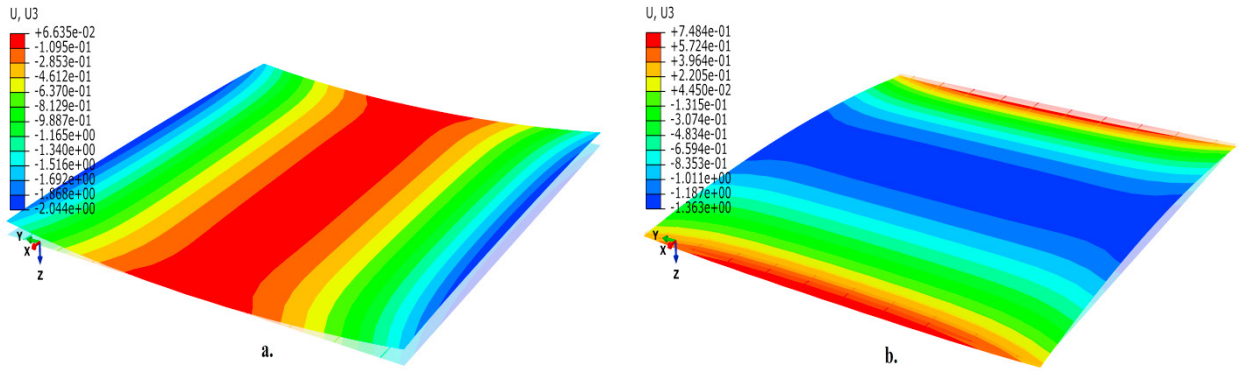

Fig. 3. Bistable Laminate: a) 1st Cylindrical Shape; 2nd Cylindrical Shape.

This number and size of wires (ten Nitinol wires with a diameter of 200μm each) is quite large with respect to the size and thickness of the laminate therefore manufacturing issues must be carefully evaluated in this case. However, the aim of this work is essentially to setup a model, and then the feeding of the model with other material properties, number, arrangement and size of wires to find, if possible, a solution that can be manufactured is foreseen in the next future. The result of simulation has been particularly useful in gaining a detailed insight into the distribution of longitudinal and transversal stresses in the top and bottom layers of the laminate and these insights can also be used to understand the behaviour of the layers adjacent to the mid-plane, in static stable configurations. It can be seen in Fig. 4a), 0° layer developed compressive stress of -14.49 MPa in fibre direction due to the curvature acquired by the laminate after cool-down stage. Whereas, after the actuation force (forward transformation) has been removed, the same layer is subject to stress concentrations near to the longitudinal edges: the peak tensile stress is +52.51 MPa right along the edges and +27.05 MPa in narrow regions that run longitudinally a small distance into the shell as shown in Fig. 4c). Similarly, stresses developed in 90° layer in both the statically stable shape has shown in Fig. 5a) and 5c). During actuation stage, the longitudinal contraction of embedded nitinol wires develops tensile stresses inside the laminate with a peak of +53.72 MPa as shown in Figure 4b. Note that the peripheral region of layer is under tension and the inner region under compression, these stresses mechanically elevate the potential energy of bi-stable laminate. When the potential energy rises to the potential energy threshold between stable configurations, the laminate then snaps to the 2nd stable configuration.

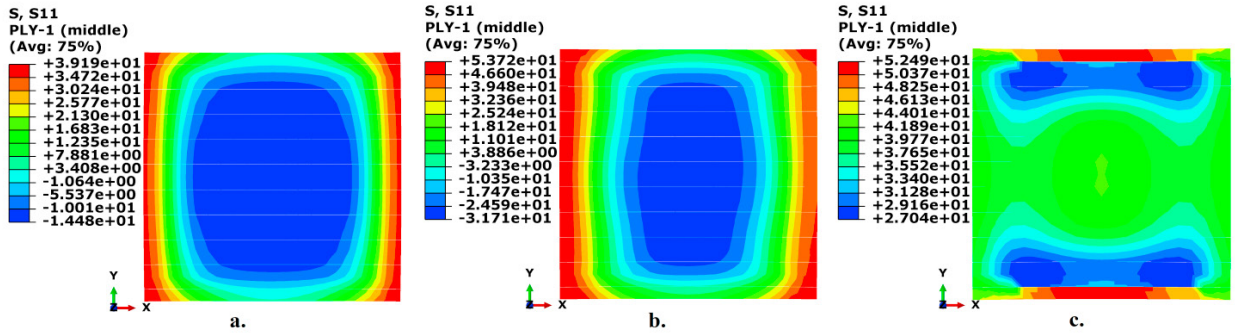

Fig. 4. S11 distribution in 0° fibre-oriented bottom layer: a) 1st Cylindrical Shape; b) Actuation stage; c) 2nd Cylindrical Shape.

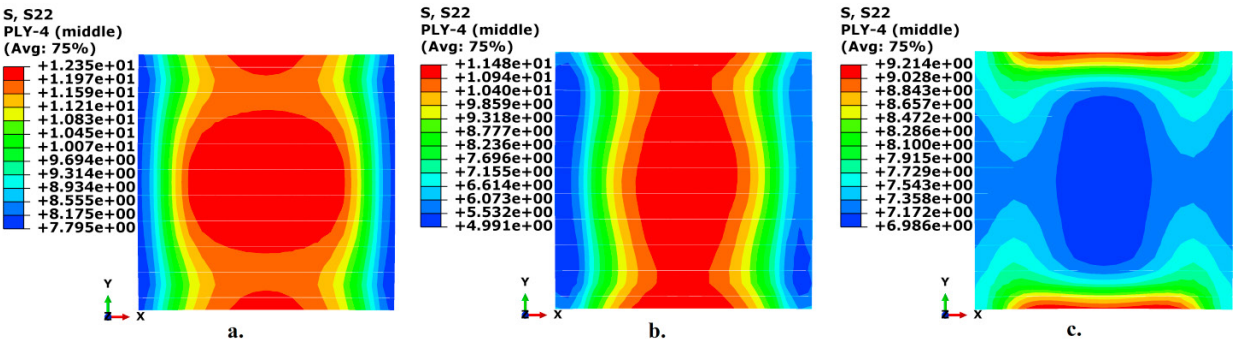

Fig. 5. S22 distribution in 90° fibre-oriented top layer: a) 1st Cylindrical Shape; b) Actuation stage; c) 2nd Cylindrical Shape

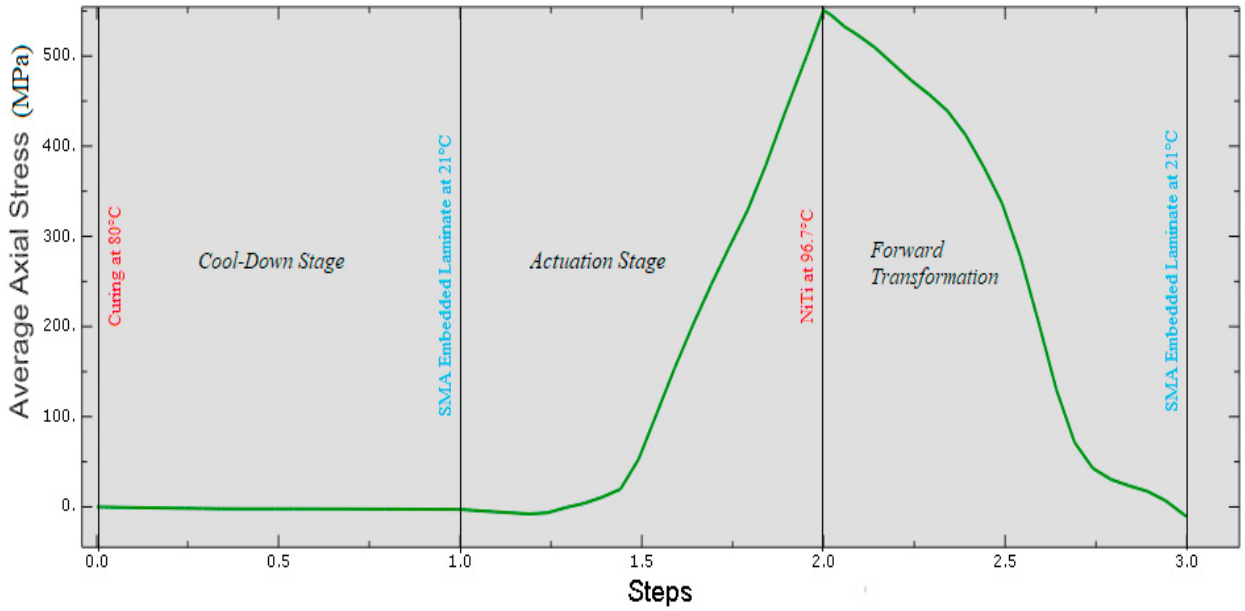

Fig. 6. Plot of average axial stress developed in Nitinol wire during various stages.

During cool-down stage, compressive stress in wires developed due to thermal contraction is about -2.84 MPa and it can be assumed to have negligible effect on laminate during curing cycle. However, tensile stress monotonically increases to a value of +550.69 MPa as the Nitinol wire temperature brought up to 96.7°C (A_f) and this dramatic change in behaviour also influence stress distribution in laminate as depicted in Fig. 4b and 5b.

5. Conclusion

From the FEA results, conclusion can be drawn out that it is possible to use SMA wires to change the shape of unsymmetric laminates. The number and size of wires found using material behaviour taken from the literature is quite large with respect to the size and thickness of the laminate, raising in turn manufacturing issues. However, based on model developed in this work, other material properties, a more versatile arrangement of SMA wire on the laminate can be tested and a detailed investigation can be done to optimize (reduce) the size and number of SMA wires necessary to obtain the actuation, to find, if possible, a solution that can be manufactured. This work is foreseen in the next future.

Acknowledgements

The work of Y. Gandhi is supported by a fellowship (assegno di ricerca) within the Ministry of University (MIUR), PRIN 2015 funded project “Smart composite laminates”.

References

Büscher, A., Radespiel, R., Streit, T., 2006. Modelling and design of wing tip device at various flight condition using a databased aerodynamic prediction tool. Aerospace Science and Technology 10, 668–678.

Dang, J., Tang, Y., 1986. Calculation of the Room-temperature Shapes of Unsymmetric Laminates. International Symposium on Composite Materials and Structures, People’s Republic of China, 201–206.

Dano, M.-L., Hyer, M.W., 2003. SMA-induced snap-through of unsymmetric fiber-reinforced composite laminates. International Journal of Solids and Structures 40, 5949–5972.

Falcã, L., Gomes, A., Suleman, A., 2009. Morphing Wingtip Devices Based on Multistable Composites, RTO-MP-AVT-168 – NATO Research and Technology Organisation Applied Vehicle Technology Panel Symposium on Morphing Vehicles. Évora, Portugal, 1–12.

Hyer, M.W., 1981. Calculations of the room-temperature shapes of unsymmetric laminates. Journal of Composite Materials 15, 296–310.

Hyer, M.W., 1981.Some observations on the cured shape of thin unsymmetric laminates. Journal of Composite Materials 15, 175–194.

Jacot, A., Ruggeri, R., Clingman, D., 2006. Shape memory alloy device and control method. U.S. Patent 7,037,076.

Jun, W.J., Hong C.S., 1990. Effect of Residual Shear Strain on the Cured Shape of Unsymmetric Cross-ply Thin Laminates. Journal of Composite Science and Technology 38, 55–67.

Jung, B.-S., Kim, M.-S., Kim, Y.-M., Ahn, S.-H., 2010. Fabrication of smart structure using shape memory alloy wire embedded hybrid composite. Materialwissenschaft und Werkstofftechnik 41, 320–324.

Koiter, W.T., 1945. On the Stability of Elastic Equilibrium. Ph.D. dissertation, Polytechnic Institute Delft, Holland [English Translation, NASA TTF-10833, 1967].

Lagoudas D.C., Shape Memory Alloys: Modeling and Engineering Applications, Springer 2008.

Mattioni F., Weaver P.M., Potter K.D., Friswell M.I., 2007. Analysis of thermally induced multistable composites. International Journal of Solids and Structures 45, 657–675.

Rogers, C.A., Robertshaw, H.H., 1988. Shape Memory Alloy Reinforced Composites. Engineering Science Preprints 25, ES P25.8027.

Ryu, J., Lee, J., Cho, M., Kim, S.-W., Koh, J.-S., Cho, K.-J., 2011. Snap-through behavior of bi-stable composite structure using SMA spring actuator, 52nd AIAA/ASME/ASCE/AHS/ASC Structures, Structural Dynamics, and Material Conference. Denver CO, USA.

Schlecht, M., Schulte, K., 1999. Advanced Calculations of the Room-temperature Shapes of Unsymmetric Laminates. Journal of Composite Structures 33, 627–633.

Strelec, J. K., Lagoudas, D. C., Khan, M. A., Yen, J., 2003. Design and implementation of a shape memory alloy actuated reconfigurable wing. Journal of Intelligent Material Systems and Structures 14, 257–273.

Tawfik, S., Tan, X., Ozbay, S., Armanios, E., 2005. Anticlastic Stability Modeling for Cross-ply Composites. Journal of Composite Materials 41, 1325–1338.

Turner, T., and Patel, D., 2007. Analysis of SMA hybrid composite structure in MSC.Nastran and ABAQUS. Journal of Intelligent Material System and Structures 18, 435–447.